4698 *Macromolecules* **2010**, *43*, 4698–4707
DOI: 10.1021/ma902247y

Macromolecules
ARTICLE

A PALS Contribution to the Supramolecular Structure of Poly(L-lactide)

J. del Río,[†] A. Etxeberria,[‡] N. López-Rodríguez,[§] E. Lizundia,[§] and J. R. Sarasua*[,§]

[†]*Departamento de Física de Materiales, Universidad Complutense de Madrid, Ciudad Universitaria s/n, 28040 Madrid, Spain,* [‡]*Departamento de Ciencia y Tecnología de Polímeros and Instituto de Materiales Poliméricos (POLYMAT), Universidad del País Vasco-Euskal Herriko Unibertsitatea (UPV/EHU), M. de Lardizabal, 3. 20018, San Sebastián, Spain, and* [§]*Departamento de Ingeniería Minero-Metalúrgica y Ciencia de los Materiales, Universidad del País Vasco-Euskal Herriko Unibertsitatea (UPV/EHU), ETS de Ingeniería de Bilbao, 48013, Bilbao, Spain*

Received October 9, 2009; Revised Manuscript Received April 16, 2010

ABSTRACT: Positron annihilation lifetime spectroscopy (PALS) was conducted to follow the evolution of free volume during crystallization of PLLA at 100 °C. A finite lifetime distribution of three components was used to fit the PALS spectra. The analysis of the longest lifetime component (τ_3) indicates that the free volume distribution evolves during crystallization by increasing the number of holes yet decreasing their size; moreover, the free volume fraction increased during crystallization. Following the evolution of the shortest components a correlation was found with crystalline and amorphous phase contents present in PLLA. The first component (τ_1) was assigned to positron annihilation in occupied zones of the crystalline phase whereas the second component (τ_2) was attributed to annihilation by different amorphous arrangements. A model for the supramolecular arrangement of PLLA chains was devised in terms of free volume enlargement for annealed samples. According to this model transformations occur in mobile amorphous phase (MAP) and rigid amorphous phase (RAP) with PLLA chains evolving from folded or coil conformations in the as-quenched samples containing uniquely MAP to opener (more extended) conformations in samples containing larger RAP and crystalline fractions. The proposed model provides a rational for the understanding of some unexpected effects associated with free volume that have been observed in several semicrystalline polymer systems, i.e., the lowering of density during crystallization (dedensification), the acceleration of polymer chains dynamics around the T_g (dynamic fragility) due to a rigid amorphous phase confined by crystallites, and also the gas permeability behavior in terms of solubility and diffusion coefficients.

Introduction

Poly(L-lactide) (PLLA) is a semicrystalline biodegradable polymer of increasing use in medical applications such as temporary implants or scaffolds for tissue engineering. The biomedical applications are highly dependent on biodegradation rate of PLLA that can be tuned by the crystalline and amorphous phases developed during the manufacturing processes. PLLA is known to yield nearly full amorphous structure when thermoplastic conformation is carried out by quenching from the melt state to temperatures below the glass transition temperature (T_g). However, as a result of its chain stereoregularity, PLLA develops partial crystallinity if a subsequent annealing treatment is conducted above T_g, or also when during conformation a nonisothermal solidification of the melt is carried out at mild/low cooling rates.[1,2]

A semicrystalline polymer can be considered as a heterogeneous material whose amorphous fraction displays different behaviors depending on the dimensions and location of the disordered domains with respect to the crystalline phase. Amorphous chains characterized by different mobility have been observed by calorimetry and relaxation experiments in semicrystalline polymers such as polyethylene,[3,4] isotactic and syndiotactic polypropylene,[5,6] polyamide 6,[7] poly(ethylene terephthalate) (PET),[8] poly(butylene terephtalate) (PBT),[9,10] poly(phenylene sulphide) (PPS),[11,12] polycarbonate,[13] poly(hydroxybutyrate) (PHB)[14] or poly(L-lactide).[15,16] The loss of segmental mobility of the amorphous phase, termed rigid amorphous phase (RAP), due to coupling to crystals causes in PLLA a decrease of the specific heat capacity and an increase and broadening of the glass transition temperature in regard to the bulk mobile amorphous phase (MAP), and hence can be quantitatively assessed by thermal analysis.[16,17]

The dimensions of the crystalline−amorphous regions and the magnitude of the immobilization of the amorphous phase probably are controlled by chain architecture that fixes the inherent flexibility of the macromolecule and by the structure and amount of the crystal surfaces that can be adjusted within limits by properly choosing the conditions of crystallization. In this work we have chosen poly(L-lactide) as model polymer to conduct an isothermal crystallization conditioning after melt quenching in order to tune its crystalline and amorphous phases.

The crystalline fraction (χ_c) and both amorphous MAP (χ_{MA}) and RAP (χ_{RA}) fractions were determined by thermal analysis and X-ray diffraction (WAXS). The crystalline morphology and the nature of the lamellar structure, with indication of whether spherulites are space filling or not, was studied by polarized Atomic Force Microscopy (AFM) in order to asses the appropriate distribution of RAP and MAP according to the existing models. The heterogeneous stack model (HEM) considers the entire MAP located at the interspherulitic boundaries and hence RAP is located between adjacent lamellae within spherulites. Contrarily, for the homogeneous stack model (HSM) the MAP is placed between the lamellae within

*Corresponding author. E-mail: jr.sarasua@ehu.es.

 Published on Web 04/28/2010

spherulites and hence RAP is assumed in the occluded space between spherulites.[7]

Early works by Galeski et al[18,19] focused on the boundary regions between spherulites observing cavities that resulted because of the confinement of the melt in a buildup of negative pressure. The presence of cavities between spherulites was confirmed in polypropylene, high-density polyethylene and other semicrystalline polymers. The occluded areas of the interspherulitic regions were called "weak spots" since holes and cavities act as stress concentrators leading to brittle failure in semicrystalline polymers.[20] In this context it is worthy to note that the PALS results studied in the present work are applicable to the changes associated with the free volume during RAP formation in both possible locations, intraspherulitic according to HEM, and interspherulitic according to HSM.

In a recent work,[16] some of us reported that crystallinity and RAP formation not only elevated the T_g in regard to the bulk amorphous polylactide, but also increased the dynamic fragility of polylactide chains. Although impediments for segmental mobility can be associated with a T_g enlargement in polymeric systems, our results showed also that the steepness or easy with which polymer chains relax on cooling to form a glass around the T_g increased with crystalline confinement; this behavior denotes a more fragile liquid and suggests an eventual increase of free volume of the rigid amorphous phase.

Schick et al.[21] considered that the amorphous constrained chains are vitrified in the state corresponding to the crystallization temperature, T_c, thus the free volume of the RAP should be notably larger than that of MAP vitrified at considerably lower temperatures.[22] Moreover, quenching of glassy polymers from the melt state is a usual method to enhance the formation of microvoids.[23] The larger free volume of the RAP has been demonstrated using positron annihilation spectroscopy (PALS)[24] and also combining PALS with pressure-volume-temperature (PVT).[25] Indeed, some authors proposed alternative ways to quantify RAP and MAP fractions based on PALS data.[24,26] Also, permeability measurements[22,27] can allow the detection of the RAP. In the case of poly(ethylene naphthalate) (PEN), free volume parameters obtained from PALS have not revealed any substantial difference between amorphous, cold- or melt-crystallized and oriented semicrystalline samples. However, oxygen transport properties of these samples allowed detecting a different accessible free volume of the amorphous phase in crystalline samples.[27]

Positron annihilation spectroscopy (PALS) gives account of free volume characteristics in polymer materials (see ref 28 for a complete review), hence we have used PALS to deepen into the PLLA supramolecular structure. When a positron enters a solid it can be annihilated after a thermalization process, with the electrons of the medium, or it can be also formed a bound state ($e^+ - e^-$) named positronium (Ps). The positronium is basically formed in two states, 75% as orthopositronium (*o*-Ps) with parallel spins (triplet state) and 25% as parapositronium (*p*-Ps) with antiparallel spins (singlet state). Parapositronium annihilates intrinsically (i.e., annihilation between the particles forming the Ps) mainly into two γ-rays of 511 keV. The lifetime of *p*-Ps is very short and has a value of 120 ps in vacuum. However, orthopositronium annihilates in vacuum into three γ-rays in order to conserve spin with a lifetime of 142 ns.[29] Into the solid, the positron wave function overlaps with electrons outside the positronium. The annihilation with such electrons having an antiparallel spin decreases the lifetime by about 2 orders of magnitude and amounts of about 1 to 5 ns. This process, with results in two γ-rays, is called pick-off annihilation and provides a sensitive measure of polymer properties associated with free volume.[30,33] The observed lifetime of the *o-Ps* depends on the positron ($\rho_+(r)$) and electron ($\rho_-(r)$) densities at the region where the annihilation takes place in the form,

$$\tau_{o\text{-Ps}} = \frac{A}{\int p_+(\vec{r})p_-(\vec{r})\,d\vec{r}} \quad (1)$$

where A is a normalization constant. A semiempirical equation can be used to approach the solution to the last equation in function of the hole size considering a model in which one Ps particle is located in a spherical wall with radius R having an infinite potential barrier.[34] This semiempirical approach assumes a homogeneous electron layer with a thickness of ($\Delta R = R_0 - R$) inside the wall, where R_0 is the infinite spherical potential radius and R is the hole radius. That hypothesis conduces to the following equation for the *o*-Ps lifetime in function of the hole radius,

$$\tau_{o\text{-Ps}} = \frac{0.5}{1 - \frac{R}{R_0} + \frac{1}{2\pi}\sin\left(\frac{2\pi R}{R_0}\right)}\ (\text{ns}) \quad (2)$$

Nakanishi et al.[35] have determined the value of ΔR by fitting the observed lifetimes with the known hole and cavity sizes in molecular substrates. The best fitted value of ΔR was found to be 1.66 Å.

When positrons are injected in polymers they can annihilate in several stages. These stages are present in the positron annihilation spectra with some components shorter than the *o*-Ps lifetime. Some authors[36,37] have summarized various possibilities for these short components (τ_1 and τ_2). The origins of these shorter lifetimes have not been firmly established, yet they could be associated with the annihilation of positrons in different regions other than the free volume, these are crystalline and amorphous regions and crystalline/amorphous interphases. Some authors[38] have evidenced in different semicrystalline polymers that Ps is formed and annihilated only in the free volume. However many works can be found in the literature relating the lifetime and intensity of *o*-Ps to different characteristics other than free volume, for example molecular weight, cross-linking, crystallinity, mechanical properties, etc.[30,37,39,40] Nonetheless, in our opinion these relations between *o*-Ps lifetime parameters and the aforementioned polymer properties do not evidence that *o*-Ps annihilate in regions other than free volume.

The evolution of the parameters associated with free volume during polymer crystallization carrying with it RAP formation is not well understood yet; hence, specific investigations with different polymers and novel strategies seem necessary to reveal the macromolecular superstructure of semicrystalline polymer systems. In this framework it should be noted that the pioneering work of Olson et al.[24] was prompted by a study of oxygen permeability in semicrystalline poly(ethylene terephtalate) (PET) revealing that the gas solubility was reduced but not in direct proportion with the decrease in amorphous volume content. The strategy devised to control the structure showed that in *cold-crystallized samples,* having higher rigid amorphous fraction for a specific crystallinity degree, τ_3 was longer (greater hole volume) and I_3 was smaller (fewer number of holes) than in *melt-crystallized* samples. The permeability results reported evidence to conclude that the dominant free volume parameter controlling the diffusion process was the hole volume whereas the dominant parameter controlling the solubility was the hole density.

PALS computations of free volume hole size and the values of positron annihilation lifetime intensities for MAF and RAF provide values evolving with crystallization conditions. For example, as crystallization progressed on PET[24] a decrease of *o-Ps* intensities (I_3) and free volume were observed in *melt-crystallized*

and *cold-crystallized* samples; with respect to *o-Ps* lifetime (τ_3), a decrease with crystallinity was observed in *cold-crystallized* samples whereas a constant value was found in *melt-crystallized* samples. In another example, as a result of the analysis of poly(3-hydroxybutyrate-*co*-3-hydroxyvalerate)[41] both I_3 and free volume decreased with crystallinity while τ_3 lifetime increased up to a crystallinity of 68% and then decreased for higher crystallinity degrees. Finally, studies on poly(tetrafluoroethylene) (PTFE) and of its copolymer with perfluoro (propyl vinyl ether) (PFA),[25] suggested that the RAF presented distinctly smaller specific free and total volume than the MAF. One may conclude from this latter study that RAF contains more holes than MAF. In conclusion, the free volume aspects related to conformational changes occurring during polymer crystallization have not been established yet and new investigations seem necessary with semicrystalline polymers presenting different chain rigidity and hence the ability to develop crystalline and rigid amorphous phases.

Moreover, PALS contributions to free volume in semicrystalline polymers have until now only focused on the interpretation of the third component. In this work we have found some interesting results for the two first components of PALS spectra, for which the studies are scarce in polymer science. Prompted by a study of polylactide chain dynamics that revealed an acceleration of segmental dynamics when traversing the T_g, due to the chain confinement by crystallites in the rigid amorphous fraction,[16] the aim of this work is to analyze the different positron annihilation lifetimes in a PLLA system in order to contribute to the understanding of the supramolecular structure of semicrystalline polymers, particularly when PALS results are interpreted in terms of free volume changes associated with mobile and rigid amorphous phases during polymer crystallization.

Experimental Section

Sample Preparation and Thermal Treatments. For this study PLLA with an average number molecular weight (M_n) of 153 000 g/mol and a polydispersity index (M_w/M_n) of 1.38, as determined by GPC, Biomer (Germany), was employed. It contains 2% D-lactyl moieties and 0.2% residual monomer, according to the supplier.

PLLA pellets were dried overnight in a vacuum oven at 30 °C prior to processing and afterward conformed in sheets of 100 mm ×100 mm ×1 mm in a hydraulic hot press by compression molding at 180 °C under a pressure of 4 bar for the first minute and 240 bar for additional 4 min. Solidification was carried by moving away the sheet from the mold and sinking it in a water bath (water-quenching, WQ). The compression-molded sheets were cut in smaller sheets of 10 mm ×10 mm ×1 mm, and were annealed in an oven. Thermal treatments were carried out at 100 °C during 2, 4, 10, 15, 30, and 60 min in order to obtain samples containing different crystalline and rigid amorphous fractions.

Positron Lifetime Measurements. Positron annihilation measurements were carried out on PLLA samples using a ^{22}Na positron source deposited onto a thin Kapton foil. This positron source was enveloped with two identical PLLA samples of 1 mm thickness. Positron lifetime spectra were recorded at room temperature using a conventional fast−fast nuclear spectrometer with a time resolution (fwhm) of 230 ps. For every measurement the average of three spectra with 2×10^6 total counts were registered and analyzed using the program PATFIT-88.

Differential Scanning Calorimetry. Differential scanning calorimetry (DSC) was conducted on a DSC 2920 thermal analyzer from TA Instruments. All scans were carried out in hermetic aluminum pans under a nitrogen atmosphere for a sample weight of approximately 5 mg. The analysis procedure consisted of a heating scan from 0 to 250 °C at a heating rate of 10 °C/min. During the scans the glass transition, cold crystallization, crystallization just before melting and melting transitions could be observed.

The fractions of crystalline (χ_c), mobile amorphous (χ_{MA}), and rigid amorphous (χ_{RA}) phases in PLLA were determined according to a procedure described in a previous work[16] with eqs 3−5

$$\chi_c = \frac{\Delta H_m - (\Delta H_{c1} + \Delta H_{c2})}{\Delta H_m^0} \quad (3)$$

$$\chi_{MA} = \frac{\Delta C_p}{\Delta C_p^0} \quad (4)$$

$$\chi_{RA} = 1 - \chi_c - \chi_{MA} \quad (5)$$

where ΔH_m, ΔH_{c1}, and ΔH_{c2} are the experimental values of melting enthalpy, cold crystallization and crystallization just before the melting of PLA crystals; ΔH_m^0 is the theoretical value of melting enthalpy for perfect PLLA crystals taken as 106 J/g,[42] and (ΔC_p) and (ΔC_p^0) are the experimental specific heat changes at T_g of PLLA and PDLLA respectively, the later giving account for the specific heat change at T_g of the nonconfined mobile fully amorphous phase ($\Delta C_p^0 = 0.639$ J/(g K)).[43]

X-ray Diffraction. In order to follow the evolution of the crystallinity with the thermal treatment, grazing incidence X-ray diffraction (GIXRD) measurements were performed on every sample. Cu Kα radiation in a Bragg−Brentano−Soller configuration was used in a Siemens diffractometer and the 2θ angle was scanned from 8° to 40° in steps of 0.04°.

Atomic Force Microscopy. The samples for the crystal morphology studies by AFM were prepared using in a first instance the solvent casting technique with chloroform (Panreac). The polymer was dissolved at a concentration of 1 wt % at room temperature and the resulting solutions were deposited into a Petri-dish and dried at 30 °C for 24 h in an oven. In order to prevent the binding of the sample with the glass substrate, Petri-dishes were covered by a thin film of PTFE. After obtaining the as-cast films, a small sample was cut and adhered to a AFM mounting disk and introduced in an oven and heated to 210 °C in order to erase previous thermal history, melt the film and evaporate any residual solvent. This temperature was maintained for 3 min and then the melted films were introduced in a preheated oven at the desired T_c crystallization temperature (80, 100, 120, 140, and 150 °C). Images of spherulitic morphology were obtained in the samples after completion of crystallization. The desired crystallization conditions were obtained by holding each sample at its crystallization temperature for 900 min and then by quenching to −10 °C; hence, any further development of the semicrystalline structure of PLLA was prevented. In order to erase any effect of the surface on the crystallization of PLLA, films of 50 ± 5 μm were used.

Atomic force microscopy (AFM) images of isothermally melt-crystallized PLLA films were recorded at room temperature using a Nanoscope IIIa Multimode Scanning Probe Microscope (Veeco Instruments, Santa Barbara, CA). The V531r1 program was employed for determining both spherulite size and spherulite density. All experiments were carried out in contact mode. The characteristic force constant of the Si_3N_4 cantilever was approximately 0.58 N/m. Scan rate of images was 2 Hz resolutions of 256 × 256 data points were used for all scans.

Results

Positron Lifetime Results. Positron lifetime spectra in polymer materials generally contain multiple exponential decay components. In the literature discrete lifetime analysis by three or four components are common to fit the lifetime spectra of polymers usually presenting a positron lifetime component longer than 1 ns that is attributed to *o*-Ps annihilation in interstitial free volume of crystals.[25,44] In

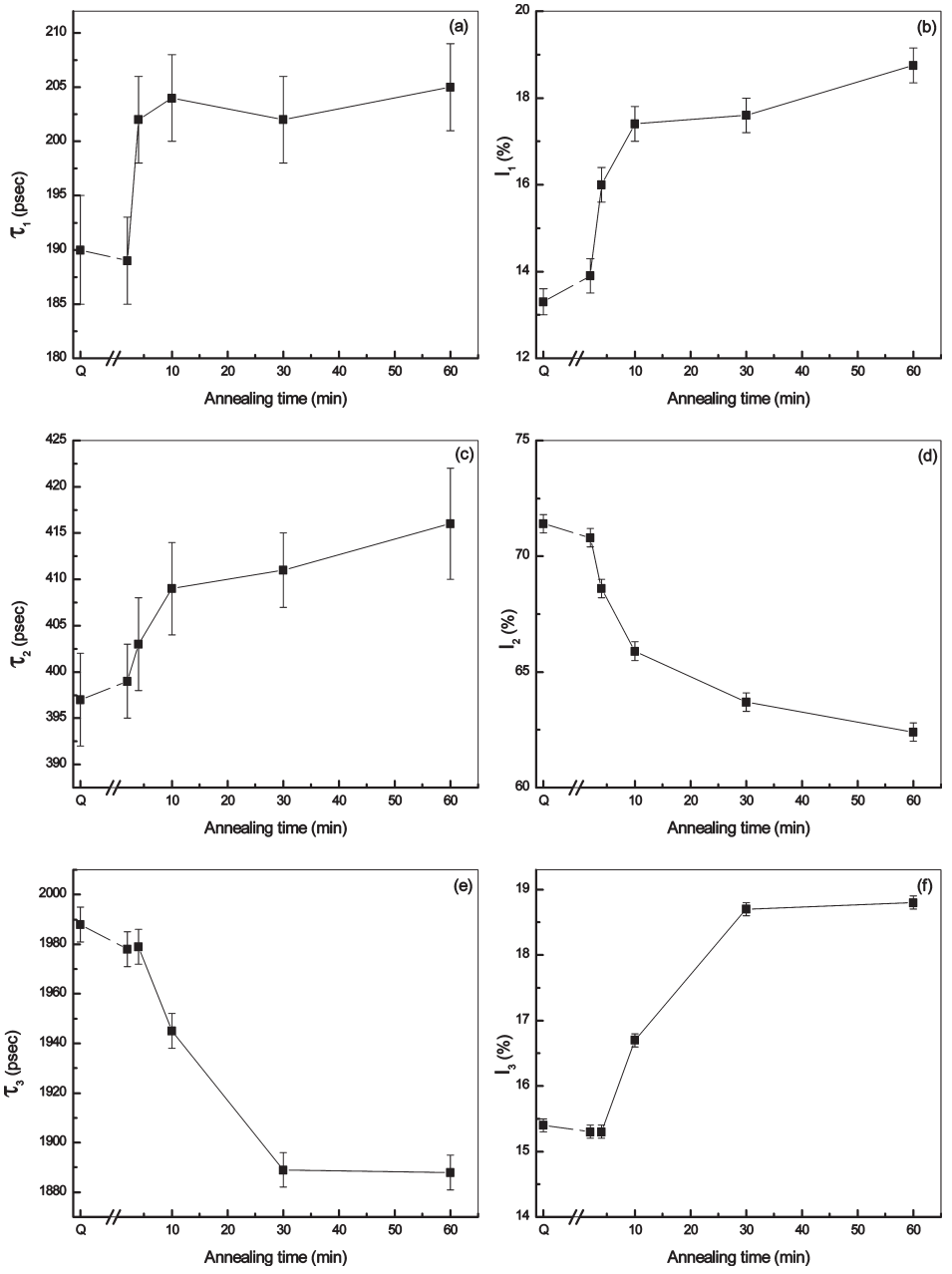

Figure 1. Positron annihilation lifetime parameters for the PLLA samples as an evolution of the annealing time at 100 °C. Q corresponds to the as-quenched sample.

the present work three and four component fittings have been explored for all samples. Good fittings were obtained for both types of analyses. The lifetime parameters (lifetime and intensity decays) obtained from a four components analysis had too much dispersion with the annealing time; however fitting the spectra with three components gave significant and physically meaning evolutions in the positron annihilation parameters with the annealing time. Hence, three components fitting was used in the analysis of our PALS spectra.

Parts a−f of Figure 1 show the evolution of positron lifetimes and intensities during the course of PLLA crystallization by annealing at 100 °C. In all cases, the length of the error bars corresponds to the difference between the maximum and minimum values obtained. The lifetime long component τ_3 has an initial value of 1990 ps in the as-quenched sample and falls down to 1890 ps after 30 min annealing. The intensity I_3 remains constant at 15.3% for 4 min, and then monotonously increases up to reaching a constant 18.8% value at 30 min.

For the first component τ_1 the value at 2 min is nearly 190 ps, which is the value measured for the as-quenched sample. For longer annealing times a significant step is observed and the 202 ps value obtained at 4 min remains approximately constant until 60 min. The intensity of the first component I_1 rapidly increases between the as-quenched state and 10 min up to 17.5%, after that a slower increase is observed reaching 20% at 60 min.

The second component τ_2 monotonously increases from 397 ps in the samples annealed during 2 min to a value of 416 ps in the samples treated for 60 min. As for the intensity of the second component, I_2 decreases from 71% in the as-quenched sample to 63% in the 60 min annealed sample.

Scanning Differential Calorimetry Results. Figure 2 shows the DSC curves of PLLA samples after conformation by water quenching and annealing at 100 °C. The as-quenched

sample shows a distinct glass transition with a heat enthalpy change at T_g = 60.6 °C followed by an exothermal deviation of the baseline indicating cold crystallization at 113.4 °C; finally a melting endotherm centered at 173.3 °C is observed. The DSC curves corresponding to the 2 and 4 min annealed samples follow qualitatively the same trends of the as-quenched sample showing T_g, cold-crystallization and melting peaks located in similar positions, yet with a small increase of the crystalline fraction in the 4 min annealed sample (Table 1). The samples annealed at 10, 15, 30, and 60 min showed a less prominent heat capacity change at the glass transition and an enlargement of crystallinity with annealing time. In addition these samples showed another deviation of the baseline at higher temperatures than the cold crystallization, this is an exothermal event suggesting a recrystallization of the existing structure giving rise to crystals of higher perfection just before the melting.[45]

Table 1 summarizes the thermal properties obtained by DSC. It is noted that the T_g significantly increases with annealing time, from 60.6 °C obtained in as-quenched PLLA to a maximum value of 66.8 °C in PLLA annealed for 30 min. It can be noted that the continuous decrease in the heat enthalpy change with annealing time does not quantitatively correspond with the increase observed in the crystalline fraction. This result suggests the existence of a rigid amorphous phase and will be discussed later on.

The results obtained for the fractions of crystalline (χ_c), mobile amorphous (χ_{MA}) and rigid amorphous (χ_{RA}) phases in PLLA samples calculated according to eqs 3−5 can also be read in Table 1 and Figure 5. Assuming that PDLLA with ΔC_p^0 = 0.639 J/(g K) at T_g contains uniquely mobile amorphous phase corresponding to the fully amorphous polymer, the reduced heat enthalpy change observed in PLLA indicates the coexistence of both MAP and RAP. Finally, it is observed that when quenched in water PLLA gives an inconsiderable crystalline fraction and RAF and therefore it can be considered nearly amorphous. However, after quenching, annealing of PLLA increases monotonously the crystalline and rigid amorphous fractions until reaching respectively the values of 36.5% and 48.5% after a 60 min annealing time.

X-ray Diffraction Results and Atomic Force Microscopy. In order to corroborate how the thermal treatment affects the crystalline fraction and morphology of PLLA X-ray diffraction and atomic force microscopy analysis was carried out. Figure 3 shows the X-ray diffraction spectra vs annealing time. In order to compare the spectra profiles the data have been normalized to the total area under the diffractogram. The as-quenched sample and the sample annealed for 2 min showed only a smooth distribution corresponding to the amorphous halo. The X-ray diffraction profile of samples annealed for 4 min or longer times showed the characteristic diffraction peaks of semicrystalline PLLA. Diffraction peaks appear progressively as the crystalline fraction develops at 2θ values of 14.6°, 16.5°, 18.8°, and 22.1°. The most intense peak at a 2θ = 16.5° is due to reflections from (200) and/or (110) planes. Less intense peaks are also observed at 2θ = 14.6°, 18.8°, and 22.1° corresponding respectively to reflections of (010), (203), and (015) planes. These results are in close agreement with the peaks reported in the literature for the α polymorph of polylactide.[42,46]

Figure 4 shows the height images of PLLA obtained in the atomic force microscope after melt quenching and isothermal crystallization for 1 h at 100 and 120 °C respectively. Please note that despite the films were initially conformed by solvent casting they were subsequently mounted in an AFM probe and melted in an oven previously to their crystallization at the selected temperature. Taking into account that thin films of 50 μm produced by solvent casting were quenched from melt state in air when moving from the melting oven to the crystallization oven, the crystallization procedure used for AFM and PALS samples are considered

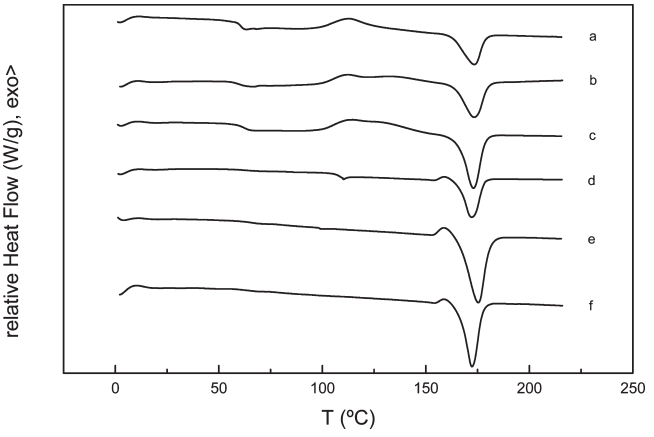

Figure 2. DSC curves of PLLA: (a) water quenched, (b) recrystallized 2 min at 100 °C, (c) 4 min at 100 °C, (d) 15 min at 100 °C, (e) 30 min at 100 °C, and (f) 60 min at 100 °C.

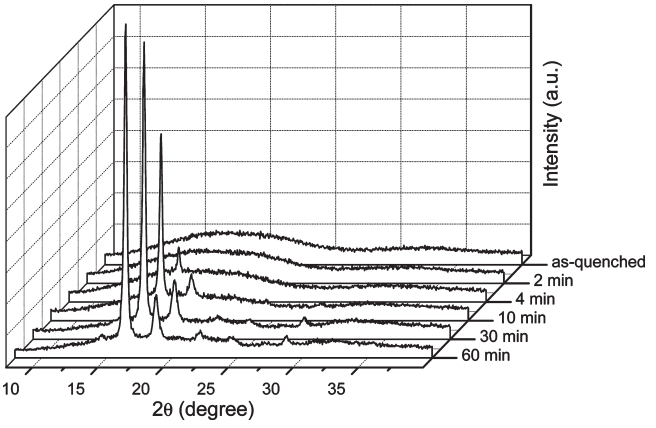

Figure 3. X-ray diffraction pattern for the PLLA samples in function of the annealing time at 100 °C. The difractograms have been normalized to the under total area.

Table 1. Thermal Properties of PLLA by DSC Including Crystalline Fraction (X_c), Rigid Amorphous Phase (X_{RA}) and Mobile Amorphous Phase (X_{MA}) after Water Quenching (WQ) and Recrystallization at 100 °C

sample	T_g (°C)	ΔC_p (J/g °C)	ΔH_{c1} (J/g)	ΔH_{c2} (J/g)	ΔH_m (J/g)	X_c	X_{RA}	X_{MA}
WQ	60.6	0.553	24.7		25.6	0.008	0.112	0.880
2 min, 100 °C	61.3	0.526	18.1		19.5	0.013	0.149	0.838
4 min, 100 °C	62.2	0.502	36.5		41.5	0.047	0.154	0.799
10 min, 100 °C	61.7	0.405	15.2	1.2	36.8	0.193	0.162	0.645
15 min, 100 °C	61.7	0.193		1.7	36.5	0.327	0.366	0.307
30 min, 100 °C	66.8	0.151		3.1	38.8	0.338	0.422	0.241
60 min, 100 °C	65.1	0.094		2.0	40.7	0.365	0.485	0.150

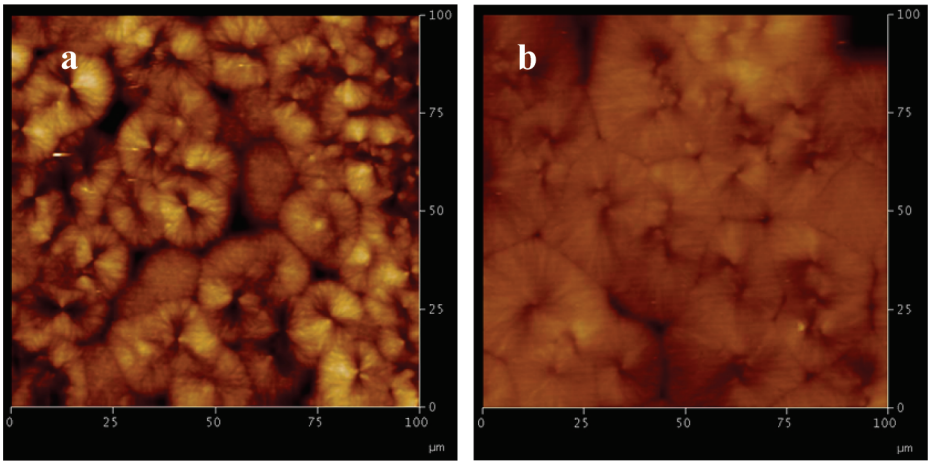

Figure 4. AFM height images of PLLA quenched from the melt and isothermally crystallized at (a) 100 °C and (b) 120 °C.

Table 2. Spherulite Diameter and Nucleation Density of PLLA Samples Quenched in Water from the Melt and Recrystallized at Different Crystallization Temperatures (T_c)

T_c (°C)	spherulite diameter (μm)	nucleation density (mm^{-2})
80	7	30000
100	16	4335
120	40	2400
150	142	50

equivalent, being at the time similar to that termed *melt-crystallization* in another work.[24]

The AFM images reveal spherulitic morphology close to space filling confinement in both cases. Table 2 reports a monotonous increase in spherulite diameter from 7 μm after completion of crystallization at 80 °C to 142 μm at 150 °C. In addition, the nucleation density monotonously decreases from 30000 to 50 mm^{-2} as crystallization temperature increases from 80 to 150 °C (Table 2). Hence, AFM analysis reveals that average size diameter increases when PLLA crystallization is performed at lower undercoolings from the melt and is leaded by a lowering of nucleation density. The changes observed during the treatment follow the results reported in the literature for recrystallization studies in polymer films.

Discussion

Previous comments have delineated the fact that the structure of semicrystalline polymers requires the consideration of a three phase model including a crystalline phase, a noncrystalline amorphous phase and a crystalline−amorphous interphase. In polymers crystallizing with spherulitic morphology the rigid amorphous phase has been associated with the presence of topological constraints induced by confining lamellae that radially grow as stacks from a spherulite nucleus. Interlamellar regions are separated by amorphous layers (20−40 Å) while much thicker mobile amorphous layers separate the spherulites from one another (100−2000 Å).[47,48] From this point of view, it has been proposed that RAP is associated with the interlamellar thin regions. In addition, it is accepted that RAP does not contribute to the jump of heat capacity; hence, only the MAP regions participate in the glass transition.[49]

Differences in the mobility and free volume between RAP and MAP can be analyzed by different methods such as calorimetry, relaxation, free volume or permeability measurements. It is also well established that free volume, particularly the size of the holes,[25] plays an important role in mobility. Thus, discussion will be focused on the influence of RAP. With this aim, all the components of the positron annihilation lifetime spectrum will be analyzed in this work.

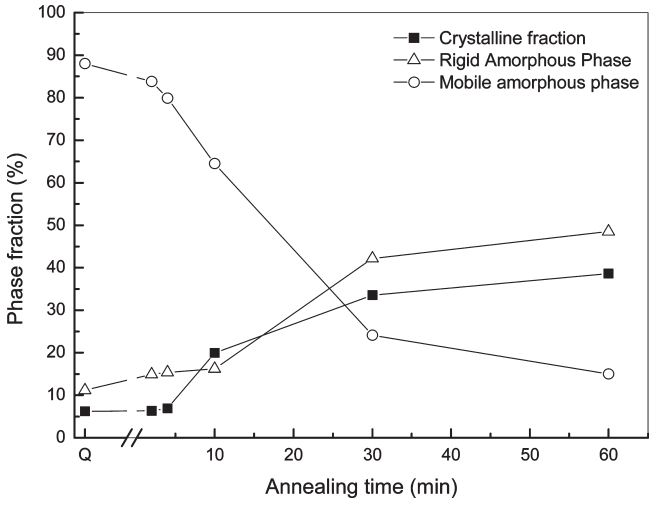

Figure 5. Crystalline, rigid amorphous and mobile amorphous phase fractions versus annealing time at 100 °C, obtained from scanning differential calorimetry results. Q corresponds to the as-quenched sample.

Figure 5 shows the evolution of crystallinity together with the rigid amorphous and mobile amorphous fractions of PLLA versus annealing time. It deserves being emphasized here the fact that the crystalline development in PLLA during annealing carries with it not only an enlargement of the T_g but also the presence of a rigid amorphous fraction, since larger values of χ_{RA} correspond to larger χ_c values.

The third component of PALS spectra, corresponding to the pick off annihilations of *o*-Ps is related to the free volume. In semicrystalline polymers, it is widely assumed that the free volume is principally located in the amorphous regions and not in the more dense crystal regions.[24] Furthermore, we have not observed in our PLLA samples the extra *o*-Ps lifetime observed in some semicrystalline polymers.[25,44]

Since RAP is vitrified at crystallization temperature (T_c), the free volume characteristics should be different in RAP and MAP. At T_c, the interlamellar RAP has a reduced mobility while the MAP has a rubbery character featured by micro-Brownian segmental motions.[50] Thus, it can be expected that both amorphous phases to possess different free volume hole size and distribution for MAP and RAP. In this work, due to the limited resolution of positron spectra, the data corresponding to the third

components τ_3 and I_3 will be considered as an average of both amorphous phases[25,26] and the observed evolution for τ_3 and I_3 will be analyzed taking into account the relative amounts of RAP and MAP.

The values of τ_3 correspond to the pick off annihilations of *o-Ps* present in PLLA and the relative intensity I_3 accounts for the number of free volume holes. This positron state is formed in free volume regions and a mean radius of the free volume hole can also be determined by means of eq 2. Hence, the decrease of τ_3 with annealing time should be associated with a size decrease of free volume holes. According to the calculations, the free volume hole size (v_f) ranges from 95.7 Å^3 in the as-quenched sample to 86.5 Å^3 in the 60 min annealed sample. It deserves to be noted that all analysis has been performed using a discrete term fitting. Since I_3 increases with annealing time, the calculated hole size value decreases as the amount of free volume holes increases. Hence, according to this analysis, an evolution to smaller but higher quantity of holes results as a consequence of the thermal treatment at 100 °C, in comparison to the as-quenched state.

Olson et al.[24] conducted PALS measurements on PET samples quenched from the melt and recrystallized at 110 and 210 °C for samples termed *cold-crystallized* and *melt-crystallized* respectively. The results indicated that crystallization yields a decrease in I_3 for both *cold-crystallized* and *melt-crystallized* samples. However, a decrease of τ_3 with crystallinity was only observed in *melt crystallized* samples while in *cold crystallized* samples τ_3 remained practically constant. The evolutions of I_3 and τ_3 PLLA observed in Figure 1 for PLLA agree with the above-mentioned trends observed for *melt-crystallized* PET. This result is noticeable since PLLA samples investigated in this work were crystallized at a temperature with a melt undercooling approximately the same of that used for the above-mentioned *melt-crystallized* PET samples.

On the basis of χ_{RA}, χ_{MA}, and τ_3 and I_3 variations, some numerical estimations of free volume magnitudes in RAF, i.e., $\tau_{3,RAF}$ and $I_{3,RAF}$, have been carried out.[24] Our computations with PLLA resulted in values of $I_{3,MAF} = 14\%$, $\tau_{3,MAF} = 1990$ ns, $I_{3,RAF} = 36.5\%$ and $\tau_{3,RAF} = 1904$ ns. These differences between RAF and MAF free volume parameters are in agreement with previous results obtained for *melt-crystallized* PET.[24] Also, the larger value for $I_{3,RAF}$ agrees too with Dlubek et al.,[25] who suggested that RAP should contain a higher amount of holes than MAP.

The fraction of free volume (f_v) is defined by the ratio of the free volume to the total volume,

$$f_{v00} = \frac{V_f}{V_t} \tag{6}$$

where $V_f = V_t - V_o$ and V_o is the occupied volume. In the studies of polymers, it is useful to determine changes in this parameter in order to relate it with different physical properties like diffusion or mechanical properties. The probability of *o*-Ps annihilation is assumed to be proportional to the number of free volume holes and the free volume fraction, f_v, can be determined by using the following equation,[51,52]

$$f_v = CI_3 v_f(\tau_3) \tag{7}$$

where v_f is the free volume hole size determined as above-mentioned by eq 2 and C is a empirical scaling constant which is determined by other type of free volume fraction measurements. In common polymers the value of C ranges from 0.001 to 0.002 but due to the fact that it is difficult to know the C value, Hill et al.[53] have proposed to use an arbitrary average value of 0.0015. Also, Li et al.[54] have defined an apparent free volume fraction, $f_{V,app} = I_3 v_f(\tau_3)$. Also, some authors have pointed out

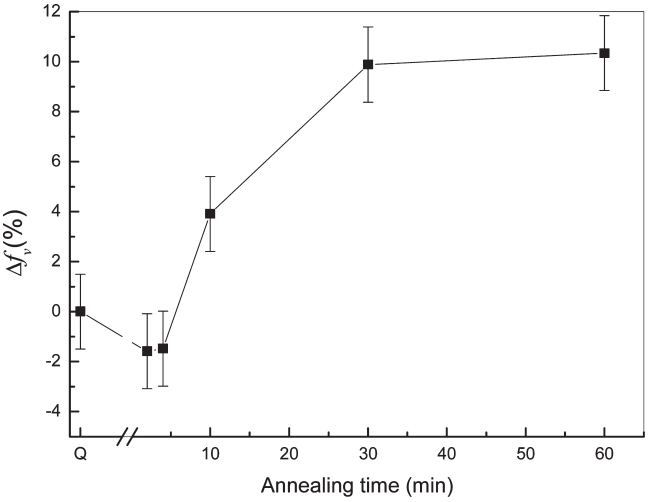

Figure 6. Free volume fraction increment for the PLLA samples in function of the annealing time at 100 °C. $\Delta f_v = (f_v^t = -f_v^Q)/f_v^Q$, where f_v^t is the free volume fraction after an annealing time of t minutes and f_v^Q is the free volume fraction in the as-quenched state.

with an argument against this relation between I_3 and f_v considering that I_3 is affected by radiation chemistry of polymeric materials.[55,56] However, eq 7 can be considered as a relative value for a polymer of the same series since it was derived on the basis of the Williams−Landel−Ferry theory.[30,57] Relative fractional free volume estimated by $f_{v,app}$ is well accepted in the literature.[24,30,58] Recently, Cheng et al. have observed a good linearity between crystallinity and $f_{v,app}$.[41] In this work, in order to obviate C and taking into account that we are more interested in the evolution of f_v with annealing than in its absolute value, we have used the free volume fraction increment, defined as $\Delta f_v = (f_v^t = -f_v^Q)/f_v^Q$, where f_v^t is the free volume fraction after an annealing time of t minutes and f_v^Q is the free volume fraction in the as-quenched state.

Figure 6 shows the evolution of the free volume fraction increment with annealing time relative to the as-quenched PLLA. As can be seen, a 2 or 4 min of annealing produces an initial decrease of free volume fraction increment; however, longer annealing times yield an increase of this quantity with respect to the as-quenched state. This last result could seem counterintuitive since the amorphous fraction and its associated free volume decreases with crystalline development. At this point of the discussion, it is worth mentioning what the density values reported for other semicrystalline polymers containing rigid and mobile amorphous phases are. Semicrystalline syndiotactic poly(styrene), for instance, presents smaller density than its fully amorphous counterpart, the latter being obtained by avoiding the crystallization by rapid solidification from the melt.[59] For poly(ethylene terephtalate), although some results for different crystallinity samples report no significant change of f_v,[24] other results have revealed for interlamellar regions containing RAF a densification thus higher f_v in terms of PALS.[60] Regarding poly(3-hydroxybutyrate-*co*-3-hydroxyvalerate), an increase of the relative fractional free volume with temperature during a thermal treatment was also reported, likely inducing recrystallization.[57]

One could also argue that PLLA lamellae and hence the crystal lattice itself may contain a significant part of the free volume to be added to the free volume of the rigid and mobile amorphous regions computing for total free volume. In this hypothesis, the possibility of a change in helical structure of PLLA could be considered as a contributing factor to the free volume. However, according to the X-ray diffraction results the α crystal form of PLLA and its parameters at 100 °C do not change with annealing time. Moreover, the density of the amorphous PLLA is inferior to

the crystalline one, 1.245 and 1.29 g/cm^3 respectively.[61] Our PALS analysis shows that both I_3 and fractional free volume (f_v) increase with crystallinity while τ_3 decreases. If the observed f_v increase was due to the increase of free volume inside the crystal lattice originated by a change of helical structure in PLLA, the larger fractional free volume observed would not agree either with the trend to higher density that is derived from the higher density of crystalline PLLA reported above or with the unchanged crystalline lattice parameters of the α crystalline lattice derived from X-ray diffraction patterns. We have measured the densities of the PLLA samples by a gradient density column, and the results obtained indicated that density was not increased with crystallinity, suggesting a smaller density for RAP. As a consequence, in the PLLA case, we discard a significant contribution of the free volume located in crystal lattices and corresponding lamellae. Hence, our results suggest that conformational changes induced by annealing in the amorphous phases of PLLA lead to a larger free volume fraction that being associated with RAP region formation exceeds the free volume reduction corresponding to the fractional increase of the lamellar crystalline regions.

Solubility of gases in glassy polymers has also been related to the free volume. Some authors have observed an enlargement of oxygen solubility due to a larger excess of free volume associated with RAF.[22,24,27,60] Diffusion processes are more sensitive to the free volume hole size as it has been observed in PET, in which the melt-crystallized samples have both lower oxygen diffusion coefficient and τ_3 in comparison to cold-crystallized ones.[24] Thus, the variation obtained for both τ_3 and f_v in this work are in good agreement with these results.

The PALS results in PLLA agree too with those recently reported by some of us in which segmental dynamics of polylactide chains covering the T_g − 30 °C to T_g + 30 °C range was studied in the absence and presence of a crystalline phase by dynamic mechanical analysis (DMA). These results, obtained using the framework provided by the WLF theory and Angell's dynamic fragility concept,[16] indicate that amorphous PDLLA is a stronger glass former than semicrystalline PLLA, hence the latter is dynamically more fragile; i.e., the conformational changes when traversing the glass transition are performed faster. Since PLLA contains also a RAP fraction these results suggest a higher free volume fraction of RAP favoring the segmental mobility of PLLA chains under crystalline confinement conditions, leading to a higher dynamic fragility in regard to fully amorphous PDLLA containing only MAP.

Throughout the bibliography the two shorter annihilation components have not been extensively discussed. For example, τ_2 has been attributed to "defects" present in the polymeric crystalline regions[36,37] as occurs in conventional crystalline materials like metals or inorganic compounds. However, in our opinion this explanation is not suitable for polymers in which the crystalline structure arrangement is formed by chain folding. Concerning to the first component, τ_1 is usually associated with the annihilation of positronium in the *p*-Ps state. As mentioned in the Introduction, *p*-Ps autoannihilate with a lifetime of 120 ps in vacuum, however τ_1 reported in the bibliography are somewhat higher than this value. Although the positron annihilation research in polymers has not usually interpreted τ_1 and τ_2 in relation to structural characteristics, we have found some interesting results for these annihilation lifetimes in annealed PLLA. In order to explain them we propose that the first and the second components τ_1 and τ_2 are related with the occupied zones of the polymer, either crystalline or amorphous.

Figure 1d shows a very remarkable high intensity values associated with the second component I_2. In the as-quenched state the crystallinity is only 5% indicating that the PLLA sample is mainly amorphous. We propose that the second component is associated with the annihilation in the amorphous zone; hence, the decrease of the intensity I_2 with annealing time would describe the progressive amorphous to crystalline transformation leading to a decrease of the intensity of the second component. As shown in Figure 1c, the increase of τ_2 from 397 ps for the as-quenched samples to 416 ps in the 60 min annealed sample suggests a transformation inside the total amorphous region (MAP plus RAP) to opener structures. The folded conformations that characterize chains in mobile amorphous phase obtained in the as-quenched samples would evolve to rigid amorphous regions in the annealed ones presenting more extended chain conformations.

The amorphous−crystalline phase transformation carries with it the formation of a rigid amorphous phase having a larger free volume fraction than the MAP due to a higher amount of free volume holes, even though the hole size is smaller (Figure 1, parts a and b). In addition the evolution of the second component τ_2 to longer values has suggested that a more extended conformation of the amorphous chains is formed during the formation of rigid amorphous phase giving rise to opener structures. The following scenario could be drawn to explain these results: the formation of new holes of free volume are produced due to the conformational changes in confined chains in regard to chains that are not confined forming mobile amorphous regions. The confined chains are located in the interlamellar or interspherulitic spaces forming a RAP or interphase of reduced mobility. Being anchored to crystals, chains in RAP are forced to take more extended conformations. Since PLLA's mobile amorphous phase at 100 °C is above its T_g, chains easily adapt their conformations to form new holes and free volume distribution. However, RAP becomes vitrified during melt crystallization at higher temperature than MAP, and because of the reduction of mobility with regard to MAP the RAP, unlike MAP, cannot reduce its free volume to values closer to those corresponding to the equilibrium state. This opener amorphous arrangement of PLLA chains in RAP explains the increase of τ_2 with the progress of crystallization during annealing.

Parts a and b of Figure 1 show the evolution of the first component parameters τ_1 and I_1. As proposed above for the second component, the increase of I_1 with annealing time suggests that this positron annihilation state is associated with the occupied crystalline phase. The results of τ_1 suggest two different stages: the former corresponding to the as-quenched and crystallization until 4 min (τ_1 takes a 190 ps value) and the latter for longer annealing times showing an almost constant lifetime value of 204 ps.

However, before the discussion of the data corresponding to the first component some comments are necessary. As mentioned in the Introduction, 25% Ps formed in the sample should annihilate in *p*-Ps state, whose lifetime in vacuum has been reported to be around 125 ps. In our case the annihilation lifetime spectrum has been properly fitted with values ranging from 190 to 205 ps, as shown in Figure 1a, yet they are attributed to the annihilation of the *p*-Ps state. Taking into account that the *p*-Ps fraction contains $^1/_3$ *o*-Ps, one could expect a partial influence of the latter on I_1. Our results show that I_3 changes from 15.5 to 18.75%, thus only a 1% of the I_1 can be attributed to the *o*-Ps contribution in *p*-Ps state. Since Figure 1b shows that I_1 ranges from 13.2% to 19%, the evolution of I_1 with annealing time will be interpreted in terms of the annihilation in the crystalline regions. Please note that although there is a clear correlation of I_1 with crystallinity, the change in I_1 cannot coincide quantitatively with the crystallinity change determined by DSC that is computed from mass fractions. PALS is sensitive not only to the occupied crystalline and amorphous regions but also to the free volume, which is not accounted for in the DSC measurements; hence, it seems not to be pertinent to establish a quantitative relation between PALS intensities and DSC crystallinity.

Assuming that τ_1 represents the annihilation of positrons in occupied crystalline zones, the τ_1 jump observed in Figure 1a after 4 min annealing suggests an increase of the crystalline cell volume and a decrease of the atomic packing density in the crystalline region. These low variations in τ_1 lifetimes have been related to dilatation phenomena in other crystalline materials.[62] Since τ_1 remains almost constant at 202 ps after 4 min, our results indicate that the crystalline phase has achieved a critical size, denoting no further structural changes in the occupied crystalline regions as crystalline fraction develops during annealing.

Conclusions

Positron annihilation lifetime spectra are sensitive to the structural complexity of semicrystalline polymers and can compliment the information provided by other techniques such as X-ray diffraction or calorimetry. The PALS analysis conducted in this work has allowed monitoring of the changes produced in the supramolecular structure of PLLA by isothermal crystallization of an amorphous sample by annealing at 100 °C. The changes in the supramolecular structure detected by PALS comprise not only those determined by the crystalline and amorphous (RAP and MAP) fractions, but also give account of the free volume and the occupied volume characteristics associated with polymer chains in crystalline and both amorphous regions.

The analysis of the third component of the annihilation spectrum (τ_3 and I_3) associated with free volume demonstrated that a lower free volume hole size and a higher number of holes were found in PLLA as RAF increased during crystallization. As a combination of both, an increase of the free volume fraction was determined, in good agreement with previous results reported on semicrystalline polymers. Some interesting trends were also observed in the first two components (τ_1 and I_1; τ_2 and I_2, respectively). Since no interpretation for these shorter lifetime components applied to polymer systems is found in the literature, a hypothesis has been proposed to be validated by further studies. According to it, the first component is associated with the annihilation in zones occupied by chain segments of the crystalline phase; here the initial increase of τ_1 is related with dilation phenomena produced in the initial stages of crystallization until a crystal critical size is achieved. Concerning the second component, it reflects the changes in the amorphous structure evolving from folded conformations to more extended conformation as RAP fraction increases.

The PALS analysis indicates that chains must adopt more extended and rigid conformations in RAP regions than in MAP regions. On a whole the PLLA crystallization process results with the formation of a large number of new holes of smaller free volume, attributed to the fact that chains are vitrified in RAP at higher temperatures than those in MAP. The results are in good agreement with the free volume data obtained by means of the third component. The analysis of the PALS results has provided a theoretical background to explain the increased gas solubility and dynamic fragility as well as the uncommon density loses reported for several polymer systems containing a rigid amorphous fraction over those containing only a mobile amorphous phase.

Acknowledgment. The authors are thankful for financial support from the Basque Government Dept. of Industry, Trade, and Tourism (Project Etortek IE07-201), from Spanish Ministerio de Ciencia y Tecnología (Projects MAT 2006-13436-C02-01 and MAT2005-03358) and from the University of the Basque Country (Projects GIC07/85-IT-274-07 and GIC07-IT-338-07). N.L.R. expresses thanks for the predoctoral fellowship from the Basque Government. J.d.R. thanks the MCYT for partial support of this work by Project FIS2007/61326.

References and Notes

(1) Miyata, T.; Masuko, T. *Polymer* **1998**, *39*, 5515.
(2) Sarasua, J. R.; López-Arraiza, A.; Balerdi, B.; Maiza, I. *Polym. Eng. Sci.* **2005**, *45*, 745.
(3) Kitamaru, R.; Horii, F.; Murayama, K. *Macromolecules* **1986**, *19*, 636.
(4) Kolesov, I. S.; Androsch, R.; Radusch, H.-J. *Macromolecules* **2005**, *38*, 445.
(5) Grebowicz, J.; Lau, S. F.; Wunderlich, B. *J. Polym. Sci., Polym. Symp.* **1984**, *71*, 19.
(6) Zia, Q.; Mileva, D.; Androsch, R. *Macromolecules* **2008**, *41*, 8095.
(7) Chen, H.; Cebe, P. *J. Therm. Anal. Calorim.* **2007**, *89*, 4.
(8) Menczel, J.; Wunderlich, B. *J. Polym. Sci., Polym. Lett.* **1981**, *19*, 261.
(9) Pyda, M.; Nowak-Pyda, E.; Mays, J.; Wunderlich, B. *J. Polym. Sci., Part B: Polym. Phys.* **2004**, *42*, 4401.
(10) Schick, C.; Wurm, A.; Merzlyakov, M.; Minakov, A.; Marand, H. *J. Therm. Anal. Calorim.* **2001**, *64*, 549.
(11) Lu, S. X.; Cebe, P.; Capel, M. *Macromolecules* **1997**, *30*, 6243.
(12) Lu, S. X.; Cebe, P. *Polymer* **1996**, *37*, 4857.
(13) Wissler, G. E.; Crist, B., Jr. *J. Polym. Sci., Polym. Phys.* **1980**, *18*, 1257.
(14) Schick, C.; Wurm, A.; Mohamed, A. *Thermochim. Acta* **2002**, *392/393*, 303.
(15) Wang, Y.; Gómez-Ribelles, J. L.; Salmerón, M.; Mano, J. F. *Macromolecules* **2005**, *38*, 4712.
(16) Zuza, E.; Ugartemendia, J. M.; Lopez, A.; Meaurio, E.; Lejardi, A.; Sarasua, J. R. *Polymer* **2008**, *49*, 4427.
(17) Magon, A.; Pyda, M. *Polymer* **2009**, *50*, 3967.
(18) Galeski, A.; Piorkowska, E. *J. Polym. Sci., Part B: Polym. Phys.* **1990**, *28*, 1171.
(19) Piorkowska, E.; Galeski, A. *J. Polym. Sci., Part B: Polym. Phys.* **1993**, *31*, 1285.
(20) Schultz, J. M. *Polym. Eng. Sci.* **1984**, *24*, 770.
(21) Schick, C.; Dobbertin, J.; Potter, M.; Dehne, H.; Hensel, A.; Wurm, A.; Ghoneim, A. M.; Weyer, S. *J. Therm. Anal.* **1997**, *49*, 499.
(22) Lin, J.; Shenogin, S.; Nazarenko, S. *Polymer* **2002**, *43*, 4733.
(23) Tsujita, Y. *Prog. Polym. Sci.* **2003**, *28*, 1377.
(24) Olson, B. G.; Lin, J.; Nazarenko, S.; Jamieson, A. M. *Macromolecules* **2003**, *36*, 7618.
(25) Dlubek, G.; Sen Gupta, A.; Pionteck, J.; Hässler, R.; Krause-Rehberg, R.; Kaspar, H.; Lochlaas, K. H. *Polymer* **2005**, *46*, 6075.
(26) Kilburn, D.; Bamford, D.; Lüpke, T.; Dlubek, G.; Menke, T. J.; Alam, M. A. *Polymer* **2002**, *43*, 6973.
(27) Hu, Y. S.; Liu, Y. F.; Zhang, L. Q.; Rogunova, M.; Schiraldi, D. A.; Nazarenko, S.; Hiltner, A.; Baer, E. *Macromolecules* **2002**, *35*, 7326.
(28) Jean, Y. C.; Mallon, P. E.; Schrader; D. M. *Principles and Applications of Positron & Positronium Chemistry*; World Scientific Publishing: Singapore, 2003.
(29) Nico, J. S.; Gidley, D. W.; Rich, A. *Phys. Rev. Lett.* **1990**, *65*, 1344.
(30) Jean, Y. C. *Microchem. Condens. Matter* **1993**, *5*, 7515.
(31) Pethrick, R. A. *Prog. Polym. Sci.* **1997**, *22*, 1.
(32) Wang, C. L.; Wang, B.; Li, S. Q.; Wang, S. J. *J. Phys. Condens. Matter* **1993**, *5*, 7515.
(33) Ramachandra, P.; Ramani, R.; Ravichandran, T. S. G.; Ramgopal, G.; Gopal, S. *Polymer* **1996**, *37*, 3233.
(34) Tao, S. J. *J. Chem. Phys.* **1972**, *56*, 5499.
(35) Nakanishi, H.; Wang, S. J.; Jean, Y. C. Positron Annihilation in Polymers. In *Positron Annihilation Studies in Fluids*, Sharma, S. C., Ed.; World Scientific Publishing: Singapore, 1988; p 292.
(36) Suzuki, T.; Oki, Y.; Numajiri, M.; Kondo, K.; Ito, Y. *J. Polym. Sci., Part B: Polym. Phys.* **1992**, *30*, 517.
(37) Nakanishi, H.; Jean, Y. C.; Smith, E. G.; Sandrecki, T. C. *J. Polym. Sci., Part B: Polym. Phys.* **1989**, *27*, 1419.
(38) Davies, W. J.; Pethrick, R. A. *Eur. Polym. J.* **1994**, *30*, 1289.
(39) Singh, J. J.; Eftekhari, A. *Nucl. Instrum. Meth. Phys. Res. B* **1992**, *63*, 477.
(40) Monge, M. A.; Díaz, J. A.; Pareja, R. *Macromolecules* **2004**, *37*, 7223.
(41) Cheng, M.-L.; Sun, Y.-M.; Chen, H. *Polymer* **2009**, *50*, 5298.
(42) Sarasua, J. R.; Prud'homme, R. E.; Wisniewski, M.; Le Borgne, A.; Spassky, N. *Macromolecules* **1998**, *31*, 3895.
(43) Pyda, M.; Bopp, R. C.; Wunderlich, B. *J. Chem. Thermodyn.* **2004**, *36*, 731.

(44) Dlubek, G.; Supej, M.; Bondarenko, V.; Pionteck, J.; Pompe, G.; Krause-Rehberg, R.; Emri, I. *J. Polym. Sci., Part B: Polym. Phys.* **2003**, *41*, 3077.
(45) Ohtani, Y.; Okumura, K.; Kawaguchi, A. *J. Macromol. Sci., Phys.* **2003**, *B42*, 875.
(46) Sarasua, J. R.; López, N.; López, A.; Meaurio, E. *Macromolecules* **2005**, *38*, 8362.
(47) Lovinger, A. J.; Hudson, S. D.; Davis, D. D. *Macromolecules* **1992**, *25*, 1992.
(48) Santa Cruz, C.; Stribeck, N.; Zachmann, H. G.; Balta Calleja, F. J. *Macromolecules* **1991**, *24*, 5980.
(49) Sauer, B. B.; Hsiao, B. S. *Polymer* **1995**, *36*, 2553.
(50) Kitamaru, R. *Adv. Polym. Sci.* **1998**; *137*, 42.
(51) Kobayashi, Y.; Zheng, W.; Meyer, E. F.; McGervey, J. D.; Jamieson, A. M.; Simha, R. *Macromolecules* **1989**, *22*, 2302.
(52) Wang, Y. Y.; Nakanishi, H.; Jean, Y. C.; Sandreczki, T. C. *J. Polym. Sci., Part B: Polym. Phys.* **1990**, *28*, 1431.
(53) Hill, A. J.; Weinhold, S.; Stack, G. M.; Tant, M. R. *Eur. Polym. J.* **1996**, *32*, 843.
(54) Li, H.-L.; Ujihira, Y.; Nanasawa, A.; Jean, Y. C. *Polymer* **1999**, *40*, 349.
(55) Dlubek, G.; Bondarenko, V.; Al-Qaradawi, I. Y.; Kilburn, D.; Krause-Renberg, R. *Macromol. Chem. Phys.* **2004**, *205*, 512.
(56) Maurer, F. H. J.; Schmidt, M. *Radiat. Phys. Chem.* **2000**, *58*, 509.
(57) Cheng, M.-L.; Sun, Y.-M.; Chen, H.; Jean, Y.-C. *Polymer* **2009**, *50*, 1957.
(58) Sun, N.; Liu, J.; Dull, T.; Yee, A. F. *J. Polym. Sci., Part B: Polym. Phys.* **2007**, *45*, 1410.
(59) Olson, B. G.; Prodpran, T.; Jamieson, A. M.; Nazarenko, S. *Polymer* **2002**, *43*, 6775.
(60) Hsu, R. Y. F.; Hiltner, A.; Baer, E. *J. Appl. Polym. Sci.* **2004**, *42*, 493.
(61) Takahashi, K.; Sawai, D.; Yokohama, T.; Kanamoto, T.; Hyon, S.-H. *Polymer* **2004**, *45*, 4969.
(62) Segers, D.; Dauwe, C.; Dorikens, M.; Dorikens-Vanpraet, L. *Appl. Phys.* **1976**, *10*, 121.